

Collective stimulated Brillouin scattering modes of two crossing laser beams with shared ion acoustic wave

Jie Qiu,¹ Liang Hao *,¹ Lihua Cao,^{1,2} and Shiyang Zou¹

¹*Institute of Applied Physics and Computational Mathematics, Beijing, 100094, China*

²*Key Laboratory of HEDP of the Ministry of Education, CAPT, Peking University, Beijing, 100871, China*

Abstract

The overlapping of multiple beams is common in inertial confinement fusion (ICF), making the collective stimulated Brillouin scattering (SBS) with shared ion acoustic wave (IAW) potentially important because of the effectively larger laser intensities to drive the instability. In this work, based on a linear kinetic model, an exact analytic solution for the convective amplification of SBS with the shared IAW modes stimulated by two overlapped beams is presented. From this solution, effects of the wavelength difference, crossing angle, polarization states, and finite beam overlapping volume of the two laser beams on the shared IAW modes are studied. It is found that a wavelength difference of several nanometers between the laser beams has negligible effects, except for a very small crossing angle about one degree. However, the crossing angle, beam polarization states, and finite beam overlapping volume can have significant influences on the shared IAW modes. Furthermore, the out-of-plane modes, in which the wavevectors of daughter waves lie in the different planes from the two overlapped beams, is found to be important for certain polarization states and crossing angles of the laser beams with the finite beam overlapping volume. This work is helpful to comprehend and estimate the collective SBS with shared IAW in ICF experiments.

PACS numbers: 52.50Gi, 52.65.Rr, 52.38.Kd

* Corresponding author: hao_liang@iapcm.ac.cn

I. INTRODUCTION

In inertial confinement fusion (ICF), the overlapping of multiple beams is common for both indirect-drive and direct-drive schemes [1, 2]. This leads to complex multibeam laser-plasma instabilities. One important example is crossed-beam energy transfer (CBET) between two beams [3–7], which can redistribute laser energy, alter drive symmetry, and modify hydrodynamic conditions. Apart from CBET, the collective stimulated Brillouin scattering (SBS) and the collective stimulated Raman scattering (SRS) of multiple beams with shared daughter waves can also be important, since the temporal growth rate and convective gain are expected to depend on the combined laser intensities. Experimentally, it is observed that the energy amplification factor increases with the number of pump beams and significant scattered light losses are produced in novel backward directions due to the collective coupling [8–12]. Thus the laser-target coupling is significantly impaired. Understanding, and in some cases mitigating these endemic processes, is essential for optimizing ICF implosions.

The shared daughter wave can be a common Langmuir/ion acoustic wave or scattered light wave, termed as the shared plasma wave (SP) mode and shared scattered light wave (SL) mode, respectively. Theoretically, the homogeneous temporal growth rate for collective SP and SL modes of multiple beams has been investigated in a general framework under fluid description [13–15]. However, for most practical cases in ICF, SRS and SBS instabilities are spatial problems [16–19], for which theoretical work for the collective modes is lacking. Although two-dimensional (2D) particle-in-cell simulations have been performed recently to study SRS of two overlapped laser beams [15, 20], the out-of-plane modes, where the wavevectors of daughter waves lie in the different planes from the plane of two overlapped beams, have not been considered, since two-dimensional simulations restrict all wavevectors in the same plane. In this work, theoretical study for the SP modes of collective SBS in convective regime is performed. By a linear kinetic model, an exact analytic solution for convective amplification of SP modes of two overlapped beams is obtained in the limit of strong damping of plasma waves and negligible pump depletion. Based on this solution, impacts of the wavelength difference, crossing angle, polarization states, and finite beam overlapping volume of the two laser beams on the collective SBS modes with shared ion acoustic wave (IAW) are studied systematically. Especially, the out-of-plane modes are discussed, which might be important in ICF experiments. This work is helpful to comprehend

and estimate the collective SBS with shared IAW in ICF experiments.

This paper is organized as follows: In Section II, the theoretical model for SP modes is presented, where an analytic solution for its convective amplification is given. In Section III, impacts of the wavelength difference, crossing angle, polarization states, and finite beam overlapping volume of two laser beams on the scattered wavelength and spatial amplification of the collective SBS modes with shared IAW are investigated, and the importance of out-of-plane modes relative to in-plane modes are also discussed. In Section IV, the conclusions as well as some discussions are given.

II. THEORETICAL MODEL FOR SP MODES OF TWO BEAMS

A. Matching geometry of the SP modes

The SRS or SBS stimulated by a single laser beam is a resonant three-wave parametric instability process where the incident wave decays into a plasma wave and a scattered wave. It occurs when the plasma wave is resonant with the ponderomotive force created by beating of the laser wave and scattered light wave, and the scattered wave is resonant with the transverse current created by beating between the laser wave and the density perturbation of the plasma wave. Thus, the phase matching condition is required,

$$\mathbf{K}_0 = \mathbf{K}_s + \mathbf{K}_{es} \quad (1)$$

where $\mathbf{K}_i \equiv (\omega_i/c, \mathbf{k}_i)$ with subscripts $i = 0, s, es$ are the four-wavevectors (comprising the wave frequency ω_i and wavenumber vector \mathbf{k}) of the laser beam ($i = 0$), scattered wave ($i = s$) and the plasma wave ($i = es$) respectively.

When there are two overlapped beams at four-wavevectors \mathbf{K}_{01} and \mathbf{K}_{02} , the beating of these two waves with a common plasma wave at four-wavevector \mathbf{K}_{es} would generate scattered waves at $\mathbf{K}_{s_1} = \mathbf{K}_{01} - \mathbf{K}_{es}$ and $\mathbf{K}_{s_2} = \mathbf{K}_{02} - \mathbf{K}_{es}$. (The anti-Stokes components are ignored here.) The coupling of these generated scattered waves with the laser beams (\mathbf{K}_{s_1} with \mathbf{K}_{02} or \mathbf{K}_{s_2} with \mathbf{K}_{01}) generates two new plasma waves at $\mathbf{K}_{es} \pm \Delta\mathbf{K}_0$, where $\Delta\mathbf{K}_0 \equiv \mathbf{K}_{01} - \mathbf{K}_{02}$. Again, the coupling of these two plasma waves with the pump beams generates two new scattered wave at $\mathbf{K}_{s_1} + \Delta\mathbf{K}_0$ and $\mathbf{K}_{s_2} - \Delta\mathbf{K}_0$, etc. Finally, a series of scattered waves at $\mathbf{K}_{s_1} + n\Delta\mathbf{K}_0$ and $\mathbf{K}_{s_2} - n\Delta\mathbf{K}_0$, and plasma waves at $\mathbf{K}_{es} \pm n\Delta\mathbf{K}_0$ ($n = 0, 1, \dots$) can be generated. However, only those plasma waves and scattered waves

with four-wavevectors nearly resonant with the natural modes are important. Assuming that \mathbf{K}_{es} , \mathbf{K}_{s_1} and \mathbf{K}_{s_2} are resonant with the natural modes, then the waves with $n \geq 1$ can be ignored when the two laser beams are incoherent in the sense that either $\Delta\omega_0$ or $|\Delta\mathbf{k}_0|$ is large enough to exceed the resonant peak widths of the natural modes of plasma and scattered waves. In such cases, each laser beam develops its scattered wave independently, and there are five coupled waves remained, including two laser waves and their corresponding scattered waves, and one common plasma wave. The five-wave matching condition can be written as

$$\mathbf{K}_{0\alpha} = \mathbf{K}_{s_\alpha} + \mathbf{K}_{\text{es}}, \quad (2)$$

where the subscripts $_{0\alpha}$, $_{s_\alpha}$ ($\alpha = 1, 2$) and $_{\text{es}}$ represent the incident wave, scattered wave and plasma wave, respectively.

The matching condition (2), together with the dispersion relation of the electromagnetic waves (EMWs),

$$\omega_{s_\alpha}^2 = \omega_{\text{pe}}^2 + c^2 \mathbf{k}_{s_\alpha}^2, \quad (3)$$

can determine \mathbf{k}_{es} as a function of $\mathbf{k}_{0\alpha}$, $\omega_{0\alpha}$, ω_{es} , and the out-of-plane angle α_\perp defined as the angle between the $(\mathbf{k}_{01}, \mathbf{k}_{02})$ -plane and the $(\mathbf{k}_{s_1}, \mathbf{k}_{s_2})$ -plane. Intuitively, the five-wave coupling geometry of SP modes is shown in Fig. 1, where the two spheres formed by \mathbf{k}_{s_1} and \mathbf{k}_{s_2} have radii $k_{s_\alpha} = \sqrt{(\omega_{0\alpha} - \omega_{\text{es}})^2 - \omega_{\text{pe}}^2}/c$ ($\alpha = 1, 2$) according to the matching condition (2) and the dispersion relation (3), and \mathbf{k}_{es} is determined by the intersection of these two spheres, which generally defines a circle in a plane perpendicular to $\Delta\mathbf{k}_0$. Different SP modes (corresponding to different points on the \mathbf{k}_{es} -circle) can be parameterized by the out-of-plane angle $-\pi < \alpha_\perp \leq \pi$, where the in-plane modes, for which \mathbf{k}_{es} , \mathbf{k}_{s_1} and \mathbf{k}_{s_2} are coplanar with \mathbf{k}_{01} and \mathbf{k}_{02} , have $\alpha_\perp = 0$ or $\alpha_\perp = \pi$.

Along this line, the wavevector of the shared plasma wave of three overlapped beams is determined by intersection between the three spheres formed by \mathbf{k}_{s_α} ($\alpha = 1, 2, 3$), which defines two points when existing. For more than three beams, a common plasma wave exists only when the intersection points between the three spheres formed by \mathbf{k}_{s_α} ($\alpha = 1, 2, 3$) happen to be located on spheres formed by other \mathbf{k}_{s_α} ($\alpha = 4, \dots$). This imposes a stringent requirement on the beam symmetry as noticed by [14]. For an indirect drive, the required beam symmetry can be satisfied only in a quite limited volume near the laser entrance hole (LEH), when the incident laser beams are angularly distributed in a highly symmetric

configuration [1]. Beyond this region, not only the beam symmetry condition is hard to be satisfied, but also the overlapping volume of multiple beams drops rapidly. Consequently, compared to multiple beam overlapping, effects of two beam overlapping would become more important.

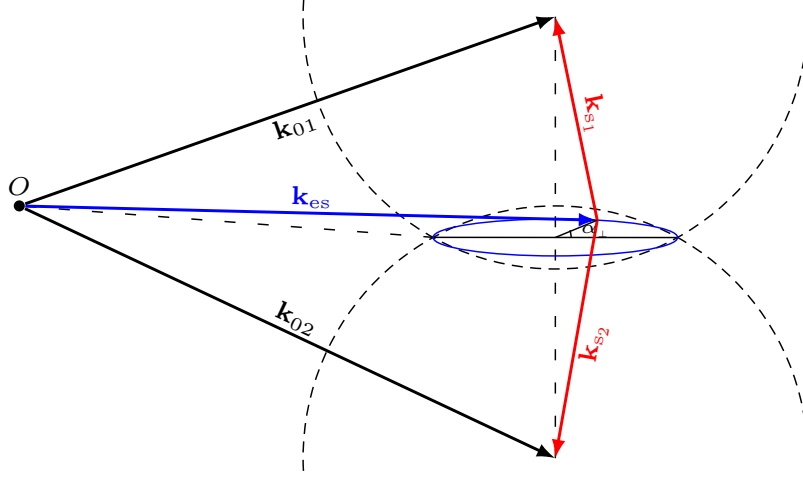


FIG. 1: The sharing of one common plasma wave by two overlapping beams (the general case with nonzero wavelength difference is demonstrated). The incident wave, scattered wave and the plasma wave are shown in black, red, and blue, respectively. The wavevectors of the all possible shared plasma waves are located on a circle (in blue) in a plane perpendicular to $\mathbf{k}_{01} - \mathbf{k}_{02}$. The out-of-plane angle $-\pi < \alpha_{\perp} \leq \pi$ is defined as the angle between the $(\mathbf{k}_{01}, \mathbf{k}_{02})$ -plane and the $(\mathbf{k}_{s1}, \mathbf{k}_{s2})$ -plane.

B. Convective amplification of the SP modes

The equation for the EMW is

$$\partial_t^2 \mathbf{A} + c^2 \nabla \times (\nabla \times \mathbf{A}) = c^2 \mu_0 \mathbf{J}, \quad (4)$$

where \mathbf{A} is the potential vector and \mathbf{J} is the transverse current. Using the cold-fluid approximation for the transverse electron motion $m_e \mathbf{v}_e = e \mathbf{A}$, the transverse current $\mathbf{J} = -en_e \mathbf{v}_e = -e^2 n_e \mathbf{A} / m_e$, where m_e , e , \mathbf{v}_e , n_e are the electron mass, electron charge, electron quiver velocity and electron number density, respectively. Substituting \mathbf{J} into Eq. (4) and taking the normalization $\mathbf{a} = e \mathbf{A} / m_e c$ yield

$$(\partial_t^2 + \omega_{pe}^2) \mathbf{a} + c^2 \nabla \times (\nabla \times \mathbf{a}) = -\omega_{pe}^2 \frac{\delta n_{es}}{n_0} \mathbf{a}, \quad (5)$$

where $n_e = n_0 + \delta n_{es}$ is decomposed into the unperturbed electron density n_0 and the perturbed electron density δn_{es} , and $\omega_{pe} = \sqrt{e^2 n_0 / \epsilon_0 m_e}$ is the plasma frequency.

In the envelope approximation for five-wave coupling of SP modes,

$$\mathbf{a}(t, \mathbf{r}) = \sum_{\alpha=1,2} \frac{1}{2} (\tilde{\mathbf{a}}_{0\alpha} e^{j\Psi_{0\alpha}} + cc.) + \sum_{\alpha=1,2} \frac{1}{2} (\tilde{\mathbf{a}}_{s\alpha} e^{j\Psi_{s\alpha}} + cc.), \quad (6)$$

and

$$\delta n_{es}(t, \mathbf{r}) = \frac{1}{2} (\delta \tilde{n}_{es} e^{j\Psi_{es}} + cc.), \quad (7)$$

where $\tilde{\mathbf{a}}_i$ is the complex vector amplitude of EMW, $\delta \tilde{n}_{es}$ is the complex amplitude of density perturbation, and the phase $\Psi_i \equiv -j\omega_i t + j\mathbf{k}_i \cdot \mathbf{r}$ with subscript $i = 0\alpha, s\alpha, es$ for the laser wave, scattered wave and plasma wave, respectively. The envelope approximation holds when $|\nabla a_i|/|a_i| \ll k_i$, $|\partial_t a_i|/|a_i| \ll \omega_i$, $|\nabla n_{es}|/n_{es} \ll k_{es}$ and $|\partial_t n_{es}|/n_{es} \ll \omega_{es}$. Using the phase matching condition (2), equations for the electromagnetic components of $\tilde{\mathbf{a}}_i$, which satisfy $\mathbf{k}_i \cdot \tilde{\mathbf{a}}_i = 0$, can be derived from Eqs. (5-7) as

$$\begin{aligned} \mathcal{L}_{em_{s\alpha}} \mathbf{a}_{s\alpha} &= -\frac{j\omega_{pe}^2}{4\omega_{s\alpha}} \frac{\delta n_{es}^*}{n_0} \mathbf{n}_{s\alpha} \times (\mathbf{a}_{0\alpha} \times \mathbf{n}_{s\alpha}), \\ \mathcal{L}_{em_{0\alpha}} \mathbf{a}_{0\alpha} &= -\frac{j\omega_{pe}^2}{4\omega_{0\alpha}} \frac{\delta n_{es}}{n_0} \mathbf{n}_{0\alpha} \times (\mathbf{a}_{s\alpha} \times \mathbf{n}_{0\alpha}). \end{aligned} \quad (8)$$

For simplicity, the tilde in the complex amplitude is dropped in Eq. (8) and the following paper. $\mathbf{n}_i = \mathbf{k}_i/k_i$ is defined as an unit vector along \mathbf{k}_i , thus the term $\mathbf{n}_i \times (\mathbf{a}_j \times \mathbf{n}_i) = \mathbf{a}_j - (\mathbf{n}_i \cdot \mathbf{a}_j) \mathbf{n}_i$ is the projection of \mathbf{a}_j onto the plane perpendicular to \mathbf{k}_i . The operator \mathcal{L}_{em_i} is defined by

$$\mathcal{L}_{em_i} \equiv \partial_t + \frac{c^2 \mathbf{k}}{\omega_i} \cdot \nabla + \frac{c^2}{2\omega_i} \nabla \cdot \mathbf{k}, \quad (9)$$

where the $\nabla \cdot \mathbf{k}$ term arises from the plasma inhomogeneity. Then, for a steady-state convective solution in the strong damping regime of homogeneous plasma, $\mathcal{L}_{em_i} = c^2 \mathbf{k}_i \cdot \nabla / \omega_i$.

While the plasma response to the ponderomotive drive has the following expression [21],

$$\frac{\delta n_{es}}{n_0} = -\gamma_{pm} \frac{k_{es}^2 c^2}{2\omega_{pe}^2} \sum_{\alpha=1,2} \mathbf{a}_{0\alpha} \cdot \mathbf{a}_{s\alpha}^*, \quad (10)$$

where the ponderomotive response function γ_{pm} is

$$\gamma_{pm}(\omega_{es}, k_{es}) \equiv \frac{(1 + \chi_I) \chi_e}{\epsilon}, \quad (11)$$

where $\epsilon = 1 + \chi_I + \chi_e$ is the dielectric function, and $\chi_I(\omega_{es}, k_{es}) = \sum_{\beta} \chi_{i\beta}(\omega_{es}, k_{es})$ and χ_e are the ion susceptibility (summed over ion species β) and electron susceptibility, respectively. For simplicity, the flow velocity is assumed to be zero for all species in the following.

Nevertheless, the above formula can be applied to the non-zero flow case by replacing ω_{es} appearing in $\chi_{i\beta}(\omega_{\text{es}}, k_{\text{es}})$ with $\omega_{\text{es}} - \mathbf{k}_{\text{es}} \cdot \mathbf{u}_\beta$ if species β were to flow with velocity \mathbf{u}_β .

Considering the polarization states of the EMWs, the EMW complex vectors can be written as $\mathbf{a}_{s_\alpha} = a_{s_\alpha} \mathbf{e}_{s_\alpha}$ and $\mathbf{a}_{0\alpha} = a_{0\alpha} \mathbf{e}_{0\alpha}$, where \mathbf{e}_i is a unit vector along the polarization direction. Using the fact $\mathbf{n}_{s_\alpha} \cdot \mathbf{e}_{s_\alpha} = \mathbf{n}_{0\alpha} \cdot \mathbf{e}_{0\alpha} = 0$, it can be proven

$$\mathbf{e}_{s_\alpha} \cdot [\mathbf{n}_{s_\alpha} \times (\mathbf{e}_{0\alpha} \times \mathbf{n}_{s_\alpha})] = \mathbf{e}_{0\alpha} \cdot [\mathbf{n}_{0\alpha} \times (\mathbf{e}_{s_\alpha} \times \mathbf{n}_{0\alpha})] = \mathbf{e}_{s_\alpha} \cdot \mathbf{e}_{0\alpha}. \quad (12)$$

According to Eq. (8), the component of \mathbf{a}_{s_α} that can be convectively amplified is along the direction of $\mathbf{n}_{s_\alpha} \times (\mathbf{e}_{0\alpha} \times \mathbf{n}_{s_\alpha})$, so \mathbf{e}_{s_α} is parallel to $\mathbf{n}_{s_\alpha} \times (\mathbf{e}_{0\alpha} \times \mathbf{n}_{s_\alpha})$, yielding the polarization alignment factor

$$\cos \varphi_\alpha \equiv \mathbf{e}_{0\alpha} \cdot \mathbf{e}_{s_\alpha} = |\mathbf{e}_{0\alpha} \times \mathbf{n}_{s_\alpha}|, \quad (13)$$

where φ_α is the angle between $\mathbf{e}_{0\alpha}$ and \mathbf{e}_{s_α} . Then, using Eqs. (12-13), for the steady-state convective solution, Eqs. (8-10) can be simplified as

$$\begin{aligned} \frac{\delta n_{\text{es}}}{n_0} &= -\gamma_{\text{pm}} \frac{k_{\text{es}}^2 c^2}{2\omega_{\text{pe}}^2} \sum_{\alpha=1,2} \cos \varphi_\alpha a_{0\alpha} a_{s_\alpha}^*, \\ \mathbf{k}_{s_\alpha} \cdot \nabla a_{s_\alpha} &= -\frac{j\omega_{\text{pe}}^2}{4c^2} \frac{\delta n_{\text{es}}^*}{n_0} \cos \varphi_\alpha a_{0\alpha}, \\ \mathbf{k}_{0\alpha} \cdot \nabla a_{0\alpha} &= -\frac{j\omega_{\text{pe}}^2}{4c^2} \frac{\delta n_{\text{es}}}{n_0} \cos \varphi_\alpha a_{s_\alpha}, \end{aligned} \quad (14)$$

Substituting δn_{es} into equations for a_{s_α} , we get

$$\mathbf{n}_{s_1} \cdot \nabla a_{s_1} = \kappa_1 (a_{s_1} + r_a a_{s_2}), \quad (15)$$

$$\mathbf{n}_{s_2} \cdot \nabla a_{s_2} = \kappa_2 (a_{s_2} + a_{s_1}/r_a), \quad (16)$$

where $r_a \equiv a_{02}^* \cos \varphi_2 / a_{01}^* \cos \varphi_1$, and the gain coefficient for single beam α is

$$\kappa_\alpha = \text{Im}[\gamma_{\text{pm}}] k_{\text{es}}^2 |a_{01}|^2 \cos^2 \varphi_\alpha / 8k_{s_\alpha} \quad (17)$$

Eqs. (15-16) are two-dimensional in nature since \mathbf{n}_{s_1} and \mathbf{n}_{s_2} are along different directions. They can be solved for a beam overlapping volume over which the pump depletion of $a_{0\alpha}$ is negligible. It is convenient to choose a (in most cases) non-orthogonal coordinate system $\mathbf{x} = x_1 \mathbf{n}_{s_1} + x_2 \mathbf{n}_{s_2}$, in which $\mathbf{n}_{s_1} \cdot \nabla = \partial/\partial x_1$ and $\mathbf{n}_{s_2} \cdot \nabla = \partial/\partial x_2$. As derived in Appendix B, the solution can be written as

$$\begin{bmatrix} a_{s_1}(x_1, x_2) \\ a_{s_2}(x_1, x_2) \end{bmatrix} = \int_0^{x_2} \mathbf{G}_1(x_1, x_2 - \xi_2) a_{s_1}(x_1 = 0, \xi_2) d\xi_2 + \int_0^{x_1} \mathbf{G}_2(x_1 - \xi_1, x_2) a_{s_2}(\xi_1, x_2 = 0) d\xi_1, \quad (18)$$

where

$$\mathbf{G}_1(x_1, x_2) = \begin{bmatrix} G_{11} \\ G_{21} \end{bmatrix} = \begin{bmatrix} \kappa_2 \kappa_1 x_1 e^{\kappa_1 x_1 + \kappa_2 x_2} \frac{I_1[2\sqrt{\kappa_1 \kappa_2 x_1 x_2}]}{\sqrt{\kappa_1 \kappa_2 x_1 x_2}} \\ (\kappa_2/r_a) e^{\kappa_1 x_1 + \kappa_2 x_2} I_0[2\sqrt{\kappa_1 \kappa_2 x_1 x_2}] \end{bmatrix} + \begin{bmatrix} e^{\kappa_1 x_1} \delta(x_2) \\ 0 \end{bmatrix}, \quad x_1 \geq 0, x_2 \geq 0 \quad (19)$$

is the SP mode response to seed of a_{s_1} at $\mathbf{x} = 0$, while

$$\mathbf{G}_2(x_1, x_2) = \begin{bmatrix} G_{12} \\ G_{22} \end{bmatrix} = \begin{bmatrix} r_a \kappa_1 e^{\kappa_1 x_1 + \kappa_2 x_2} I_0[2\sqrt{\kappa_1 \kappa_2 x_1 x_2}] \\ \kappa_1 \kappa_2 x_2 e^{\kappa_1 x_1 + \kappa_2 x_2} \frac{I_1[2\sqrt{\kappa_1 \kappa_2 x_1 x_2}]}{\sqrt{\kappa_1 \kappa_2 x_1 x_2}} \end{bmatrix} + \begin{bmatrix} 0 \\ e^{\kappa_2 x_2} \delta(x_1) \end{bmatrix}, \quad x_1 \geq 0, x_2 \geq 0 \quad (20)$$

is the SP mode response to seed of a_{s_2} at $\mathbf{x} = 0$, where I_0 and I_1 are the zero-order and first-order modified Bessel functions of the first kind, respectively.

\mathbf{G}_1 and \mathbf{G}_2 comprise two terms. The smaller second term of \mathbf{G}_1 gives us $a_{s_1}(x_1, x_2) = e^{\kappa_1 x_1} a_{s_1}(x_1 = 0, x_2)$, and thus describes the one-dimensional (1D) amplification along x_1 -direction of the sidescatter due to beam I alone. This term can ignite the two-dimensional amplification of the SP modes. For example, from seed of a_{s_1} at $\mathbf{x} = 0$, firstly the sidescatter of beam I generates perturbations δn_{es} along the 1D straight line $x_2 = 0$; this again serves as seeds to a_{s_2} and amplified along the \mathbf{n}_{s_2} direction, generating perturbations δn_{es} over the 2D \mathbf{x} -space; finally the seeding of 2D perturbations of δn_{es} results in the amplification of both a_{s_1} and a_{s_2} over the 2D \mathbf{x} -space. The steady-state two-dimensional amplification due to sharing of plasma waves is described by the first terms of \mathbf{G}_1 and \mathbf{G}_2 , where the 2D volume $V_{\text{amp}}(\mathbf{x}) \equiv \eta_1 x_1 \mathbf{n}_1 + \eta_2 x_2 \mathbf{n}_2$ ($0 \leq \eta_{0,1} \leq 1$) participates in amplifying scattered waves from the seed at $\mathbf{x} = 0$ to the point $\mathbf{x} = x_1 \mathbf{n}_1 + x_2 \mathbf{n}_2$. At sufficient gain length $\kappa_1 \kappa_2 x_1 x_2 \gg 1$, for the first term of \mathbf{G}_1 , we have

$$\mathbf{G}_1 \approx \begin{bmatrix} \frac{\kappa_2 \kappa_1 x_1}{2\sqrt{\pi}(\kappa_1 \kappa_2 x_1 x_2)^{3/4}} e^{(\sqrt{\kappa_1 x_1} + \sqrt{\kappa_2 x_2})^2} \\ \frac{\kappa_2/r_a}{2\sqrt{\pi}(\kappa_1 \kappa_2 x_1 x_2)^{1/4}} e^{(\sqrt{\kappa_1 x_1} + \sqrt{\kappa_2 x_2})^2} \end{bmatrix} \quad (21)$$

Similar results can be obtained for \mathbf{G}_2 . So all the response components G_{11} , G_{12} , G_{21} and G_{22} have the same dominant asymptotic term $G_A \equiv e^{(\sqrt{\kappa_1 x_1} + \sqrt{\kappa_2 x_2})^2}$, which is adopted in the following illustrative analysis instead of the accurate expression for $\mathbf{G}_{1,2}$.

From the asymptotic form G_A of the SP mode response, we can define a representative gain coefficient to quantify the overall amplification ability of the SP modes. There is a direction \mathbf{n}_A parallel to ∇G_A , along which the required amplification distance is minimum (in the asymptotic sense) for the seed at a given point (e.g., $\mathbf{x} = 0$) to achieve a specific

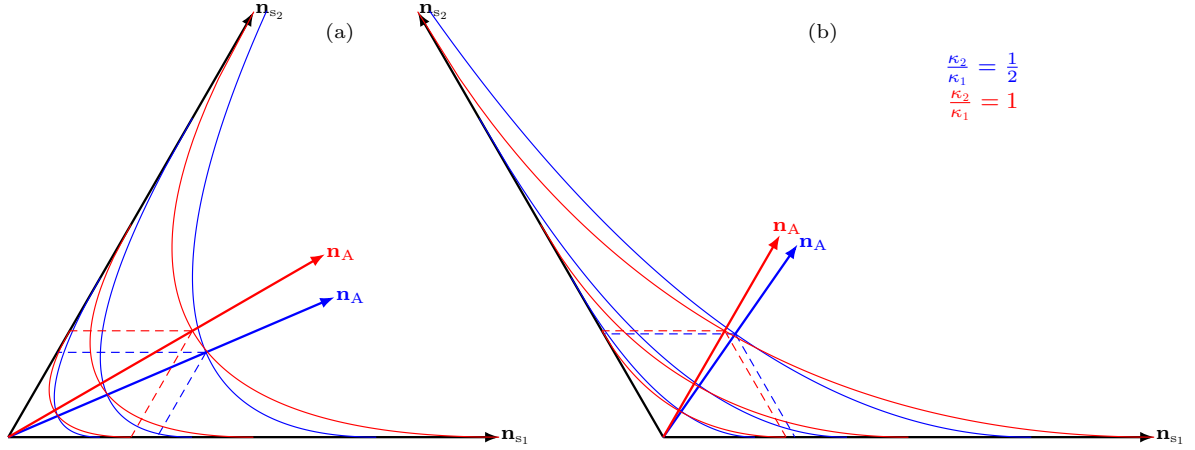


FIG. 2: The isocurves of asymptotic SP mode response $G_A = e^{(\sqrt{\kappa_1 x_1} + \sqrt{\kappa_2 x_2})^2}$ for (a) $\theta_{12}^s = 60^\circ$ and (b) $\theta_{12}^s = 120^\circ$, when $\kappa_2/\kappa_1 = 1/2$ (in blue) and $\kappa_2 = \kappa_1$ (in red). The direction \mathbf{n}_A that is parallel to ∇G is indicated. The parallelogram marked by dashed lines is the 2D gain volume that takes parts in amplifying seeds from the origin to the corresponding point.

gain, as shown in Fig. 2. The representative gain coefficient $\kappa_A \equiv \ln G_A/L_m$, where L_m is the typical size of the corresponding 2D gain volume for points along \mathbf{n}_A , can be defined as in Appendix C. In our definition, κ_A is approximately of the same magnitude as $\kappa_1 + \kappa_2$, where $\kappa_A = \sqrt{2}(\kappa_1 + \kappa_2)$ when $\kappa_1 = \kappa_2$, while $\kappa_A = \kappa_1 + \kappa_2$ when $\kappa_1 \gg \kappa_2$ or $\kappa_2 \gg \kappa_1$ such that the amplification by one beam dominates. The ratio $\mathcal{R}_A[\kappa_2/\kappa_1, \theta_{12}^s] \equiv \kappa_A/(\kappa_1 + \kappa_2)$ and the direction of \mathbf{n}_A , can be determined by κ_2/κ_1 and the angle θ_{12}^s between \mathbf{n}_{s_1} and \mathbf{n}_{s_2} , as detailed in Appendix C.

III. ANALYSIS OF SHARED IAW MODES OF TWO BEAMS

In this section, impacts of the wavelength different, crossing angle and polarization states of the two laser beams on the collective SBS modes with shared IAW are investigated. Because $k_{s_1} \approx k_{01}$ and $k_{s_2} \approx k_{02}$ for SBS, the wave coupling geometry can be simplified significantly. As shown in Figure 3, choosing point ‘O’ as the initial point, the terminal point of \mathbf{k}_a is approximately located on the circle C_a (\mathbf{k}_a -circle), which lies in the plane perpendicular to $\mathbf{k}_{02} - \mathbf{k}_{01}$, having a center located at the point ‘ O_0 ’ and a radius of the length of $|OO_0|$. According to definitions of the angles shown in Fig. 3, the relation

$$k_{01} \cos \theta_{h_1} = k_{02} \cos \theta_{h_2} = \frac{k_a}{2 \cos(\alpha_\perp/2)} \quad (22)$$

can be obtained. Defining the crossing angle between \mathbf{k}_{01} and \mathbf{k}_{02} as $\theta_{12} = \theta_{h_1} + \theta_{h_2}$,

$$k_a = \frac{2k_{01}k_{02} \sin \theta_{12} \cos(\alpha_{\perp}/2)}{\sqrt{k_{01}^2 + k_{02}^2 - 2k_{01}k_{02} \cos \theta_{12}}} \quad (23)$$

can be derived from Eq. (22).

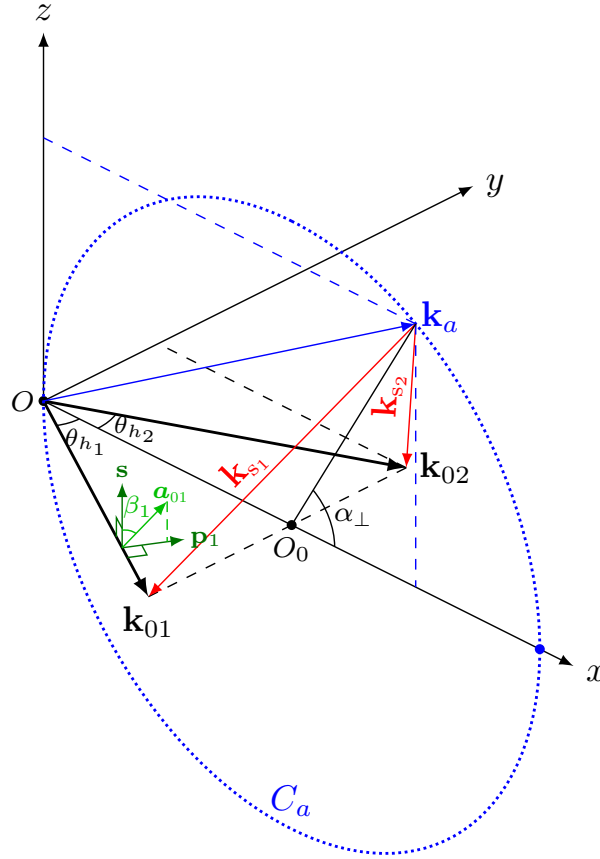


FIG. 3: The geometry of shared IAW modes of two overlapping beams. In the presented coordinate system, xy -plane is chosen to be the $(\mathbf{k}_{01}, \mathbf{k}_{02})$ -plane with x -axis perpendicular to $\mathbf{k}_{01} - \mathbf{k}_{02}$ and y -axis along $\mathbf{k}_{02} - \mathbf{k}_{01}$, and z -axis is along $\mathbf{k}_{01} \times \mathbf{k}_{02}$. The circle C_a (lying in the xz -plane), which can be parameterized by the out-of-plane angle α_{\perp} , comprises all possible locations of the endpoints of \mathbf{k}_a . Beam I or beam II is said to be s -polarized when $\mathbf{a}_{0\alpha}$ is along the $\pm \mathbf{s}$ (z -axis) direction, and p -polarized when $\mathbf{a}_{0\alpha}$ is along the direction of $\pm \mathbf{p}_{\alpha} = \pm \mathbf{s} \times \mathbf{k}_{0\alpha}$. Other linear polarization states of beam I or II are described by the polarization angle $90^{\circ} \geq \beta_{\alpha} \geq -90^{\circ}$, which is the angle from \mathbf{s} to $\mathbf{a}_{0\alpha}$.

The representative gain coefficient κ_A can be written as

$$\begin{aligned}\kappa_A &= (\kappa_1 + \kappa_2) \mathcal{R}_A[\kappa_2/\kappa_1, \theta_{12}^s] \\ &= \frac{1}{8} k_a^2 \text{Im}[\gamma_{\text{pm}}] \left(\frac{|a_{01}|^2}{k_{s_1}} \cos^2 \varphi_1 + \frac{|a_{02}|^2}{k_{s_2}} \cos^2 \varphi_2 \right) \mathcal{R}_A \left[\frac{k_{s_1} |a_{02}|^2 \cos^2 \varphi_2}{k_{s_2} |a_{01}|^2 \cos^2 \varphi_1}, \theta_{12} \right].\end{aligned}\quad (24)$$

Here $\theta_{12}^s \approx \theta_{12}$ is taken because $k_{s_\alpha} \approx k_{0\alpha}$ for SBS, and the polarization alignment factor $\cos \varphi_\alpha$ as can be calculated from Eq. (13) depends on the polarization states (β_1, β_2) of the laser beams and geometry $(\alpha_\perp, \theta_{12})$ of the SP mode. For two laser beams with the same intensity and small wavelength difference, $|a_0| = |a_{01}| = |a_{02}|$ and $k_s = k_{s_1} \approx k_{s_2}$, the upper bound of κ_A for all possible polarization combinations of the two laser beams is

$$\kappa_A^U = \frac{\sqrt{2} k_a^2 \text{Im}[\gamma_{\text{pm}}] |a_0|^2}{4k_s}.\quad (25)$$

κ_A^U can be achieved when the polarization direction $\mathbf{e}_{0\alpha} \parallel \mathbf{k}_\alpha \times \mathbf{k}_{0\alpha}$ ($\alpha = 1, 2$), which results in $\mathbf{e}_{0\alpha} \perp \mathbf{k}_{s_\alpha}$ and hence $\cos \varphi_\alpha = 1$, a complete alignment between $\mathbf{e}_{0\alpha}$ and \mathbf{e}_{s_α} .

For two overlapped laser beams with the same vacuum wavelength $\lambda_{01} = \lambda_{02}$, the \mathbf{k}_a -circle is located on the bisecting plane between \mathbf{k}_{01} and \mathbf{k}_{02} with $\theta_{h_1} = \theta_{h_2} = \theta_{12}/2$. For a non-zero wavelength difference $\Delta\lambda_0 \equiv \lambda_{02} - \lambda_{01} \ll \lambda_{01}, \lambda_{02}$, the plane in which the \mathbf{k}_a -circle lies deviates from the bisecting plane between \mathbf{k}_{01} and \mathbf{k}_{02} , with an angle

$$\Delta\theta = \frac{\theta_{h_1} - \theta_{h_2}}{2} \approx \frac{k_{01} - k_{02}}{2k_{01} \tan(\theta_{12}/2)} = \frac{\Delta\lambda_0}{2\lambda_{01} \tan(\theta_{12}/2)} \frac{1}{1 - n_e/n_c}.\quad (26)$$

From the expression for $\Delta\theta$, it can be expected that the effects of the laser wavelength difference on the SP modes are significant only when $\Delta\lambda_0/\lambda_0$ is comparable to $2 \tan(\theta_{12}/2)$. For $\Delta\lambda_0/\lambda_0 \ll 2 \tan(\theta_{12}/2)$, $\Delta\theta$ is quite small, therefore, $\theta_{h_1} \approx \theta_{h_2} \approx \theta_{12}/2$ and the dependence of \mathbf{k}_a on $\Delta\lambda_0$ is rather weak. Consequently, the effects of the laser wavelength difference on the SP modes are negligible. As an example, κ_A^U versus $\lambda_{B_\alpha} - \lambda_{0\alpha}$ are shown in Fig. 4(a) and Fig. 4(b) for $\Delta\lambda_0 = 0$ nm and $\Delta\lambda_0 = 6$ nm, respectively, where a typical plasma condition at LEH [22] $n_e = 0.06 n_c$, $T_e = 2.5$ KeV and $T_e/T_i = 3.5$ is chosen. For simplicity, the flow velocity which only leads a Doppler wavelength shift is assumed to be zero, and the gain coefficient is normalized by $I_{15} = I_{01} [\text{Wcm}^{-2}]/10^{15}$. Here, n_c is the critical density for Beam I. In Fig. 4(a), $\theta_{12} = 1^\circ$, so for $\Delta\lambda_0 = 6$ nm, $\Delta\lambda_0/\lambda_0 \approx 2 \tan(\theta_{12}/2)$. As expected, κ_A^U changes significantly when $\Delta\lambda_0$ varies from zero to 6 nm. In Fig. 4(b), $\theta_{12} = 10^\circ$, so for $\Delta\lambda_0 = 6$ nm, $\Delta\lambda_0/\lambda_0 < 0.2 \tan(\theta_{12}/2)$. As expected, the change of κ_A^U is negligible when $\Delta\lambda_0$ varies from zero to 6 nm. The small crossing angle cases with $2 \tan(\theta_{12}/2) \lesssim \Delta\lambda_0/\lambda_0$

should be of interest in the attempt to suppress laser-plasma parametric instabilities with broadband lasers [23, 24]. In most cases of ICF, the crossing angle θ_{12} is typically not too small, but the laser wavelength difference is much shorter than the vacuum wavelength [25], making its effects on the SP modes negligible. Therefore, in the following analysis, mainly the case of $\Delta\lambda_0 = 0$ is discussed for the SP modes.

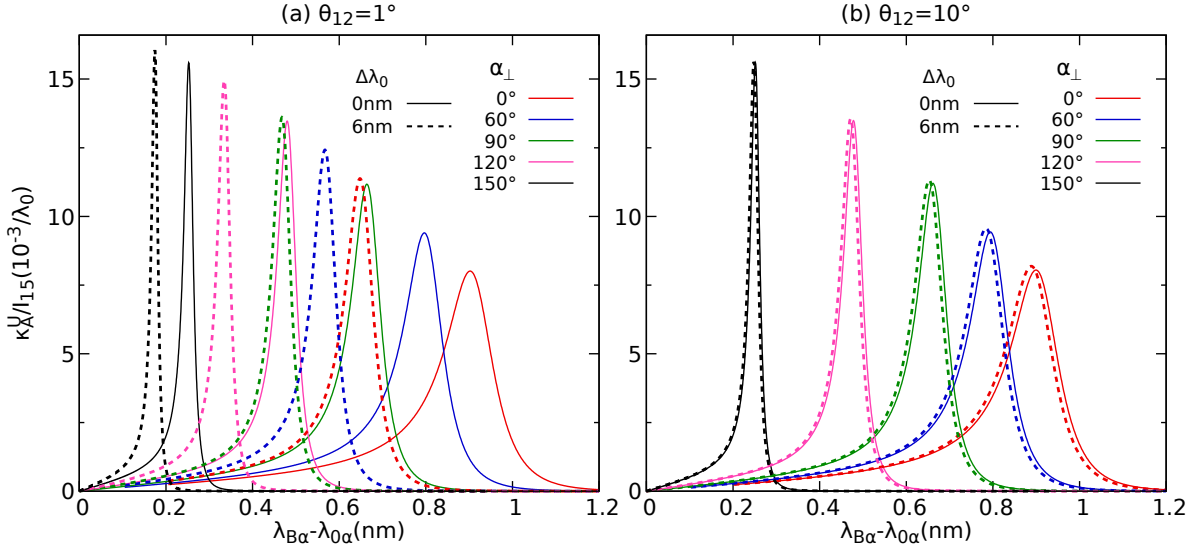


FIG. 4: κ_A^U/I_{15} versus $\lambda_{B\alpha} - \lambda_{0\alpha}$ of the shared IAW modes in He plasma for two laser beams with wavelength difference $\Delta\lambda_0 = 0$ and $\Delta\lambda_0 = 6$ nm, when the beam crossing angles are (a) $\theta_{12} = 1^\circ$ and (b) $\theta_{12} = 10^\circ$. The two laser beams are at the same intensity ($I_{01} = I_{02}$ and $I_{15} \equiv I_{01}/10^{15}$ Wcm $^{-2}$) with the vacuum wavelength $\lambda_{01} = 351$ nm and $\lambda_{02} = \lambda_{01} + \Delta\lambda_0$. The plasma condition is $n_e = 0.06 n_c$, $T_e = 2.5$ KeV, $T_e/T_i = 3.5$, and zero flow velocity.

When $\Delta\lambda_0 = 0$, Eq. (23) can be further simplified as

$$k_a = 2k_{01} \cos(\theta_{12}/2) \cos(\alpha_\perp/2), \quad (27)$$

and the scattering angle between $k_{s\alpha}$ and $k_{0\alpha}$ is

$$\theta_{\text{scat}} = \pi - 2 \arccos[\cos(\theta_{12}/2) \cos(\alpha_\perp/2)]. \quad (28)$$

In the limiting case $\alpha_\perp \sim 180^\circ$, $\theta_{\text{scat}} \sim 0$ and $\mathbf{k}_{s\alpha}$ is nearly in the forward scattering direction of $\mathbf{k}_{0\alpha}$. Such near-forward SBS needs very long time to develop, and the final saturation stage usually contains significant contribution from the anti-Stokes waves [26, 27]. Hence, we do not consider these cases here, and restrict $\theta_{12} \leq 150^\circ$ and $\alpha_\perp \leq 150^\circ$, which guarantees $\theta_{\text{scat}} > 7.6^\circ$.

Fig. 5 shows κ_A^U/I_{15} versus $\lambda_B - \lambda_0$ in He plasma for (a) SP modes with different laser beam crossing angles θ_{12} and (b) SP modes with different out-of-plane angles α_\perp , when two laser beams with the same intensity and vacuum wavelength are assumed. The scattered wavelength at which κ_A^U peaks decreases with increasing θ_{12} or α_\perp , while the corresponding peak value increases with θ_{12} or α_\perp . Since $\kappa_A^U \propto k_a^2 \text{Im}[\gamma_{\text{pm}}]$ and k_a decreases with increasing θ_{12} or α_\perp from Eq. (27), these characteristics are mainly due to properties of $k_a^2 \text{Im}[\gamma_{\text{pm}}]$, which peaks at $\omega_a \propto k_a$ and its peak value increases with decreasing k_a , as discussed in Appendix A.

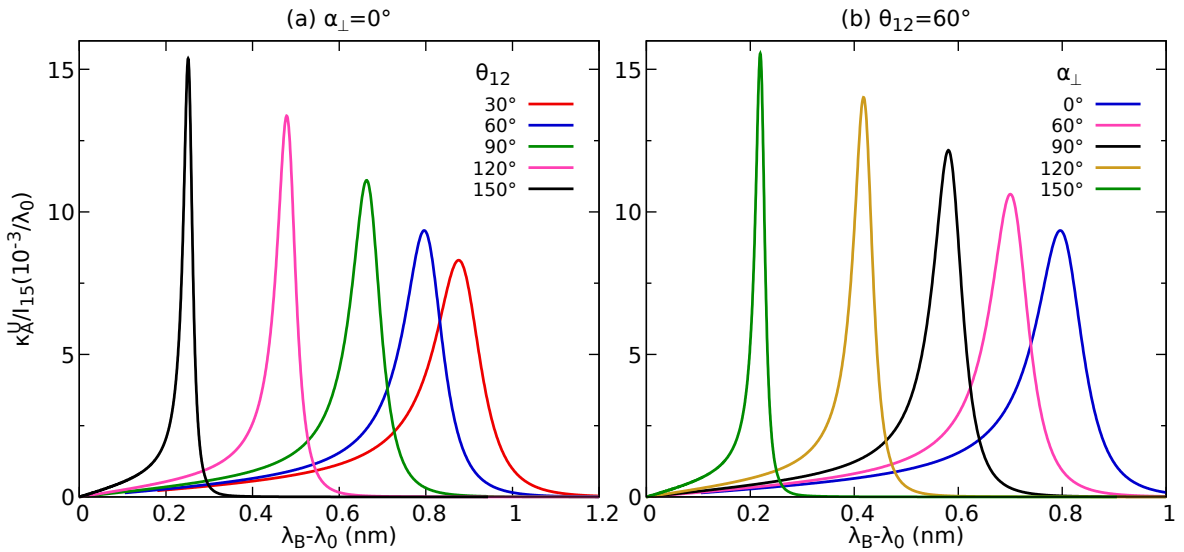


FIG. 5: κ_A^U/I_{15} versus $\lambda_B - \lambda_0$ of the shared IAW modes in He plasma for (a) $\alpha_\perp = 0^\circ$ at a variety of θ_{12} and (b) $\theta_{12} = 60^\circ$ at a variety of α_\perp . The two laser beams are at the same intensity with the same vacuum wavelength (351 nm). The plasma condition is $n_e = 0.06 n_c$, $T_e = 2.5$ KeV, $T_e/T_i = 3.5$, and zero flow velocity.

Now we consider the effects of polarization states of the laser beams on the SP mode through the dependence of κ_A/κ_A^U on different polarization combinations of beam I and beam II. For two laser beams with the same intensity,

$$\frac{\kappa_A}{\kappa_A^U} = \frac{1}{2\sqrt{2}}(\cos^2 \varphi_1 + \cos^2 \varphi_2)\mathcal{R}_A[\cos^2 \varphi_2/\cos^2 \varphi_1, \theta_{12}] \quad (29)$$

κ_A/κ_A^U depends only on the geometry $(\alpha_\perp, \theta_{12})$ of the SP mode, and the polarization alignment between the laser beams and scattered waves. The most favored SP mode by beam α , for which the polarization of laser beam and the scattered light is in full alignment

($\cos \varphi_\alpha = 1$), has $\mathbf{e}_{0\alpha} \perp \mathbf{k}_\alpha$, as discussed above. Denoting an arbitrary polarization state of the laser beam by the polarization angle β_α ($-90^\circ < \beta_\alpha \leq 90^\circ$) as shown in Fig. 3, the most favored out-of-plane angle by beam I is $\alpha_\perp = -2 \arctan[\sin(\theta_{12}/2) \tan \beta_1]$, while $\alpha_\perp = 2 \arctan[\sin(\theta_{12}/2) \tan \beta_2]$ is most favored by beam II. Except for s-polarization ($\beta_\alpha = 0$), the SP modes with non-zero out-of-plane angles are accentuated. When $\beta_1 = -\beta_2$, the polarization states of beam I and beam II are symmetric with respect to the bisecting plane between \mathbf{k}_{01} and \mathbf{k}_{02} , therefore, at one and the same α_\perp , both beam I and beam II are fully aligned with their respective scattered waves in polarization, making the value of κ_A/κ_A^U reach one for this α_\perp . For a nonzero $\beta_1 + \beta_2$, the symmetry between beam I and beam II is broken after taking into account their polarization states, the most favored out-of-plane angle α_\perp that results in a full polarization alignment between beam I and its scattered wave ($\cos \varphi_1 = 1$) deviates from the most favored α_\perp by beam II. Consequently, the maximum value of κ_A/κ_A^U labeled as $\max_{\alpha_\perp} [\kappa_A/\kappa_A^U]$ should be less than one.

Fig. 6 shows the typical variation of κ_A/κ_A^U with α_\perp for the cases $\theta_{12} = 60^\circ$ and $\theta_{12} = 120^\circ$, where effects of the degree of polarization symmetry breaking (characterized by $\beta_1 + \beta_2$) between beam I and II are illustrated in panels (a) and (c), and the overall effects of deviation from s-polarization of beam I and II (characterized by $\beta_1 - \beta_2$) are illustrated in panels (b) and (d). One remarkable feature is that different polarization states can modify the gain coefficient κ_A significantly for $|\alpha_\perp| \lesssim 90^\circ$. As a consequence, the SP mode with some out-of-plane angle, for example, the angle for which the overlapping geometry permits a long gain length, can be effectively suppressed by choosing a proper combination of β_1 and β_2 . However, for large $|\alpha_\perp|$, the modification by the polarization states becomes insignificant, because the scattering angles between $k_{0\alpha}$ and $k_{s\alpha}$ are small, and thus the polarization alignment factors $\cos \varphi_\alpha$ are less sensitive to β_α . Furthermore, it can be noticed that the polarization modification is more significant for an acute crossing angle $\theta_{12} \leq 90^\circ$ than an obtuse crossing angle $\theta_{12} > 90^\circ$. In fact, for the former, $\cos \varphi_{1,2}$ can vary from zero to one, where $\cos \varphi_{1,2} = 0$, which corresponds to a complete polarization misalignment between the laser beams and the scattered waves, occurs when $\beta_1 = -\beta_2 = \pm \arcsin[\tan \theta_h]$ and $\alpha_\perp = \arctan[(\sin \theta_h \tan \beta_1)^{-1}]$; while for the latter, $\cos \varphi_{1,2}$ can only vary from $|\cos \theta_{12}|$ to one, where the minimum of $\cos \varphi_{1,2}$ occurs when both beams are p-polarized ($\beta_1 = \beta_2 = \pm 90^\circ$) and $\alpha_\perp = 0$. Finally, there is a local maximum of κ_A/κ_A^U in the interior of our considered interval $-150^\circ < \alpha_\perp < 150^\circ$, and at this maximum the value of κ_A/κ_A^U is mainly determined

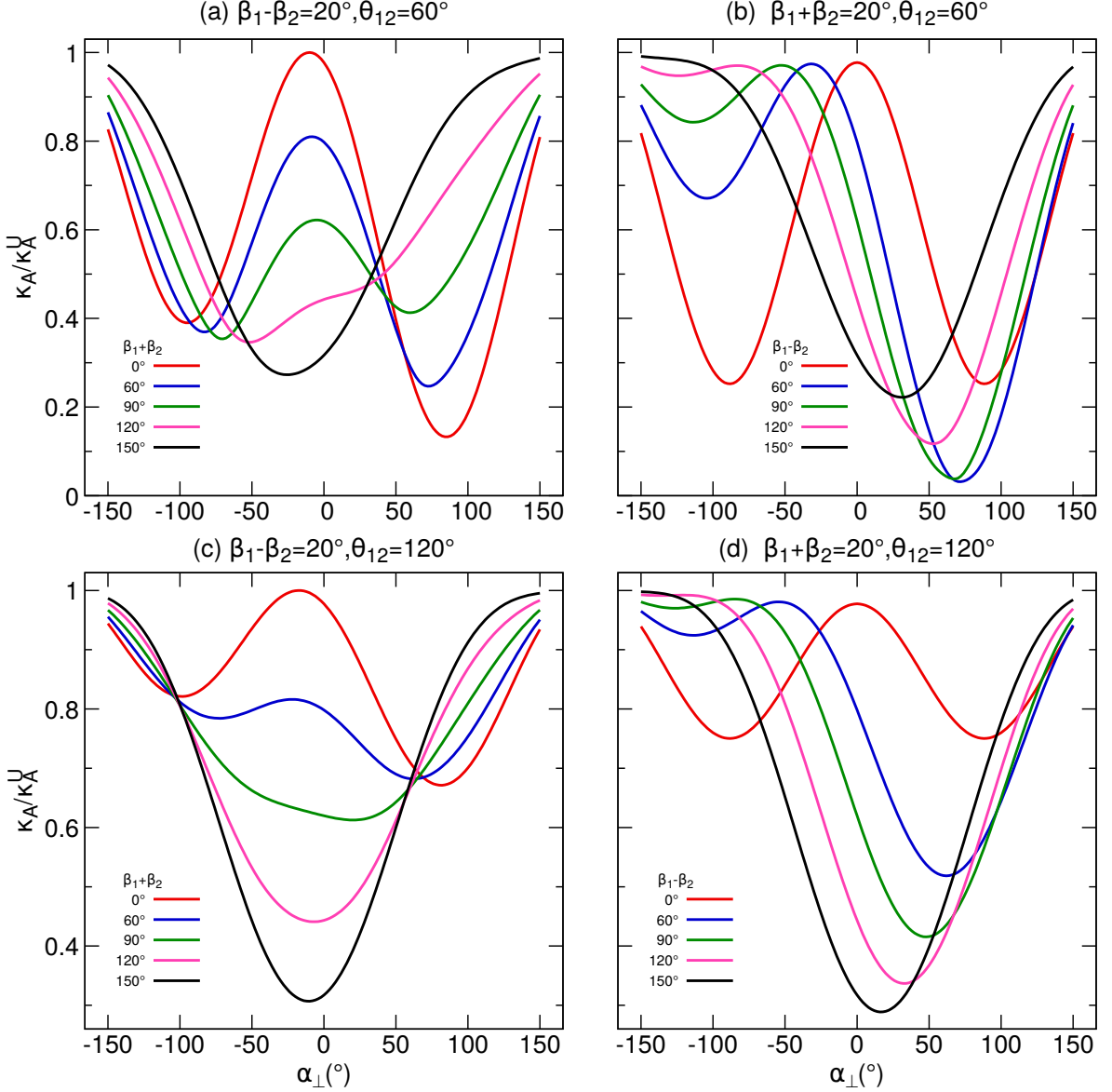


FIG. 6: κ_A/κ_A^U versus α_\perp for shared IAW modes of two laser beams with crossing angle (a-b) $\theta_{12} = 60^\circ$ and (c-d) $\theta_{12} = 120^\circ$.

by $\beta_1 + \beta_2$ (the degree of polarization symmetry breaking); while the corresponding out-of-plane angle α_\perp^M is mainly determined by $\beta_1 - \beta_2$ (the overall polarization deviation from s-polarization). The mode corresponding to the interior local maximum of κ_A/κ_A^U is of great interest, since among the SP modes with relatively small out-of-plane angles and hence large temporal growth rate $\gamma_0 \propto \sqrt{k_a} \propto \sqrt{\cos(\alpha_\perp/2)}$ [28], it is most vulnerable to be excited.

The dependence of the interior local $\max_{\alpha_\perp}[\kappa_A/\kappa_A^U]$ and its corresponding α_\perp^M on the polarization combination (β_1, β_2) is shown in Figs. 7(a,b) for case $\theta_{12} = 60^\circ$ and Figs. 7(c,d)

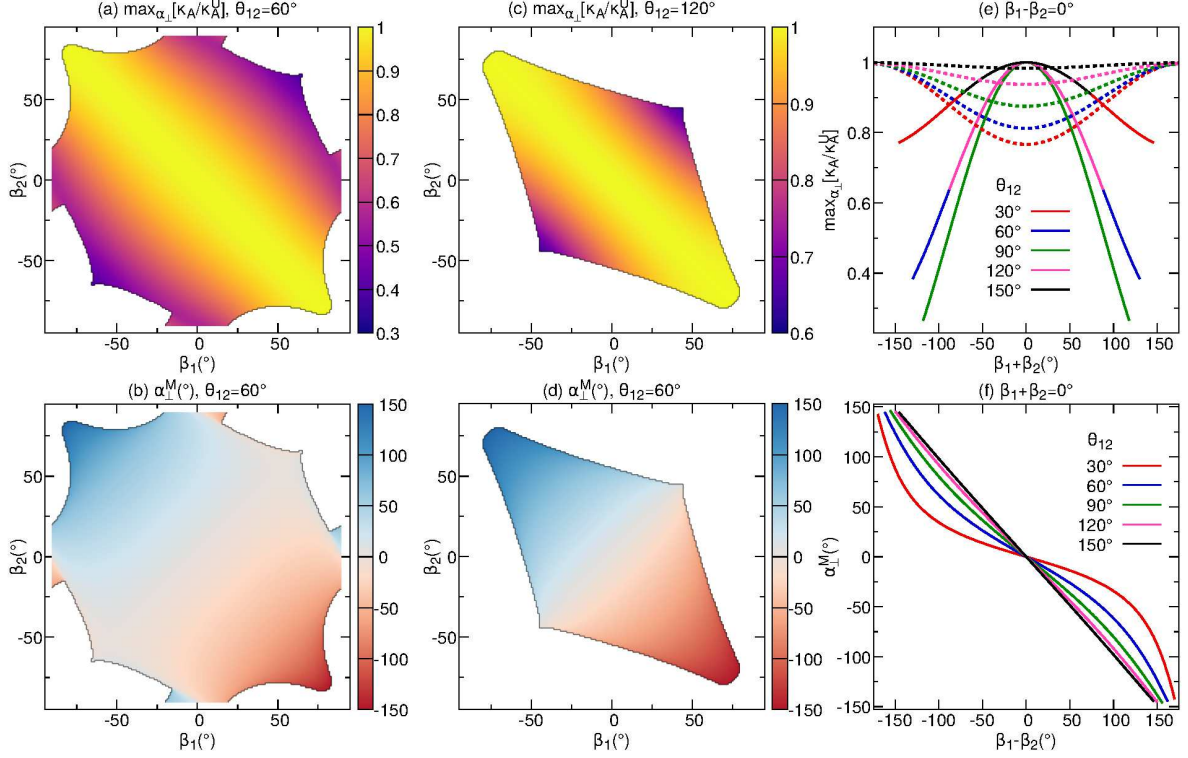


FIG. 7: (a-d) $\max_{\alpha_{\perp}}[\kappa_A/\kappa_A^U]$ and α_{\perp}^M versus β_1 and β_2 for the interior maximum of κ_A/κ_A^U when beam crossing angles are 60° and 120° . The boundary of the displayed map corresponds to (β_1, β_2) where the local maximum begins to disappear. (e) $\max_{\alpha_{\perp}}[\kappa_A/\kappa_A^U]$ versus $\beta_1 + \beta_2$ (solid curves) inside the interval $-150^\circ < \alpha_{\perp} < 150^\circ$ for different crossing angles, when $\beta_1 = \beta_2$ is taken. Notice that curves for $\theta_{12} < 90^\circ$ and for $180^\circ - \theta_{12}$ coincide except that for the former, the local maximum exists over a larger range of $\beta_1 + \beta_2$. For comparison, the larger one of κ_A/κ_A^U at the endpoints $\alpha_{\perp} = \pm 150^\circ$ is also displayed as the dashed curves. (f) α_{\perp}^M versus $\beta_1 - \beta_2$, when $\beta_1 = -\beta_2$ is taken.

for case $\theta_{12} = 120^\circ$ respectively. Fig. 7(e) shows the local $\max_{\alpha_{\perp}}[\kappa_A/\kappa_A^U]$ versus $\beta_1 + \beta_2$ (taking $\beta_1 - \beta_2 = 0$), since the local $\max_{\alpha_{\perp}}[\kappa_A/\kappa_A^U]$ is mainly determined by $\beta_1 + \beta_2$, while Fig. 7(f) shows α_{\perp}^M versus $\beta_1 - \beta_2$ (taking $\beta_1 + \beta_2 = 0$), since α_{\perp}^M is mainly determined by $\beta_1 - \beta_2$. At a small $\beta_1 + \beta_2$, κ_A/κ_A^U has a local maximum value in the interior of interval $-150^\circ < \alpha_{\perp} < 150^\circ$ as shown in Fig. 6, and this local maximum value can be larger than κ_A/κ_A^U at the endpoints $\alpha_{\perp} = \pm 150^\circ$. With the increase of $\beta_1 + \beta_2$, the interior local maximum value decreases until it disappears at some $\beta_1 + \beta_2$ as shown in Fig. 6. As a result, increasing $\beta_1 + \beta_2$ to decrease $\max_{\alpha_{\perp}}[\kappa_A/\kappa_A^U]$ for relatively small $|\alpha_{\perp}|$ can be an effective

method to suppress the collective SBS modes with shared IAW, especially for $\theta_{12} \sim 90^\circ$. On the other hand, $|\alpha_\perp^M|$ increases from zero towards 180° when $|\beta_1 - \beta_2|$ increases from zero to 180° . Therefore, due to modification of polarization states on κ_A , depending on $\beta_1 - \beta_2$ the most favored out-of-plane angle of the SP modes can deviate significantly from zero, especially for a large crossing angle. This implies the potentially important roles of out-of-plane SP modes.

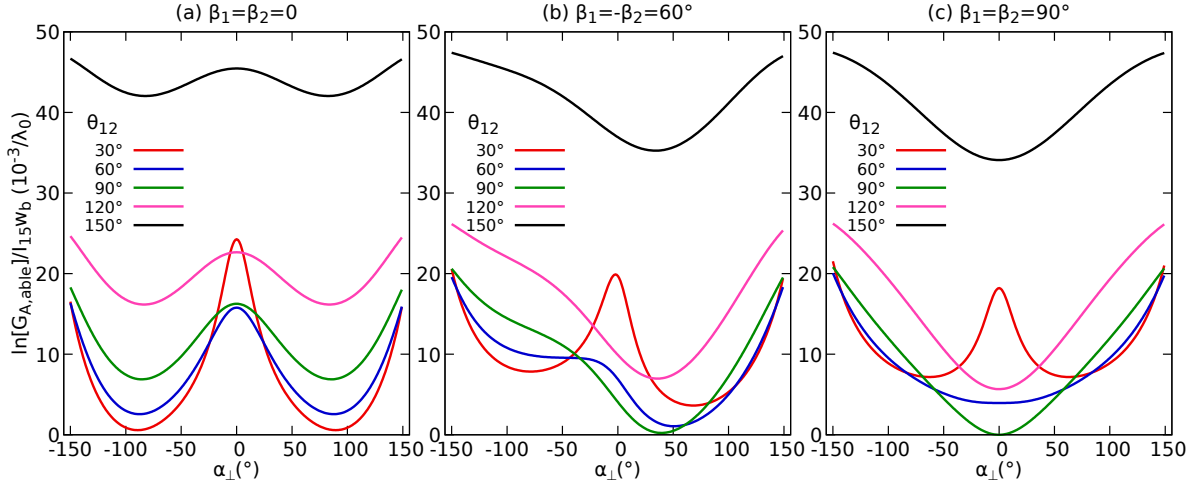


FIG. 8: $\ln G_{A,\text{able}}/I_{15}w_b$ versus α_\perp for (a) $\beta_1 = \beta_2 = 0$, (b) $\beta_1 = -\beta_2 = 60^\circ$ and (c) $\beta_1 = \beta_2 = 90^\circ$. The two laser beams are at the same wavelength (351 nm) and intensity (10^{15} W/cm 2). The plasma condition $n_e = 0.06 n_c$, $T_e = 2.5$ KeV, $T_e/T_i = 3.5$, and zero flow velocity for He plasma is taken.

In practice, the laser beam width is finite, and usually much smaller than the beam length along the laser propagation direction. Thus, a finite beam overlapping volume dependent on the width and crossing angle of the two overlapped beams is formed. For such case, the parallelogram gain volume $V_{\text{amp}}(\mathbf{x}) = \eta_1 x_1 \mathbf{n}_{s_1} + \eta_2 x_2 \mathbf{n}_{s_2}$ ($0 \leq \eta_{1,2} \leq 1$), that takes part in the amplification of the collective SP modes, must be enclosed in the beam overlapping volume. Then, the largest achievable asymptotic gain $G_{A,\text{able}}$ for the SP modes is the maximum value of $G_A \equiv e^{(\sqrt{\kappa_1 x_1} + \sqrt{\kappa_2 x_2})^2}$ subject to

$$\text{Proj}_{\perp \mathbf{k}_{01}}[V_{\text{amp}}(\mathbf{x})] \leq w_b, \quad \text{Proj}_{\perp \mathbf{k}_{02}}[V_{\text{amp}}(\mathbf{x})] \leq w_b, \quad (30)$$

where w_b is the diameter of laser beam at the overlapping point, $\text{Proj}_{\perp \mathbf{k}_{0\alpha}}[V_{\text{amp}}(\mathbf{x})]$ is the longest spatial scale of the projection of V_{amp} onto a plane perpendicular to $\mathbf{k}_{0\alpha}$, of which the calculation is given in Appendix D. The constraint condition (30) ensures the gain volume

can be enclosed within the beam overlapping region. Taking into account the finite beam width, the overlapping efficiency between the gain volume and the beam overlapping volume is highest (complete overlapping for $x_1 = x_2$) when $\alpha_\perp \sim 0, 180^\circ$ and decreases when $|\alpha_\perp|$ becomes closer to 90° . However, the decreasing speed becomes slower with the increasing crossing angle θ_{12} . It can be estimated that the overlapping efficiency decreases about 74%, 50%, 29%, 13%, and only 3% when α_\perp changes from zero to 90° , for the crossing angles of 30° , 60° , 90° , 120° and 150° , respectively. In Fig. 8, $\ln G_{A,\text{able}}/w_b I_{15}$ versus α_\perp is shown for three polarization combinations $\beta_1 = \beta_2 = 0$, $\beta_1 = -\beta_2 = 60^\circ$, and $\beta_1 = \beta_2 = 90^\circ$, where the peak values of κ_1 and κ_2 are used. For small crossing angle $\theta_{12} = 30^\circ$, the gain of in-plane modes around $\alpha_\perp \sim 0$ is always larger than the out-of-plane modes with $|\alpha_\perp| < 90^\circ$ irrespective of the beam polarization, due to the rapidly dropping overlapping efficiency with increasing α_\perp . For larger crossing angles, however, the relative importance of the out-of-plane modes with respect to the in-plane modes are determined by the beam polarization states to a greater extent. As shown in Fig. 8, with consideration of the finite beam overlapping volume, the gain of out-of-plane SP modes for large crossing angle can still be larger than the in-plane modes when either beam I or beam II deviates from s-polarization significantly. Another noticeable thing is that for a given beam width w_b , the beam overlapping region in the $(\mathbf{k}_{01}, \mathbf{k}_{02})$ -plane is a rhombus with side length $w_b/\sin\theta_{12}$, which increases with θ_{12} when $\theta_{12} \geq 90^\circ$. Together with the fact that κ_A^U increases with increasing θ_{12} as discussed above, $G_{A,\text{able}}$ at $\theta_{12} = 150^\circ$ is much larger than other crossing angles, as shown in Fig. 8. As a consequence, the larger obtuse crossing angle is beneficial to SP mode amplification. Finally, it is worth to point that the plasma inhomogeneity can result in different phase matching length along different spatial directions, imposing more limitation on the available volume that can take part in the SP mode amplification. Depending on the specific plasma condition, this can significantly modify the relative importance of different SP modes.

IV. DISCUSSION AND SUMMARY

In summary, based on a linear kinetic model for the shared plasma modes of two overlapped laser beams, an analytic convective solution is derived. From this solution, effects of wavelength difference, crossing angle and polarization states of the two beams on the collective SBS modes with shared IAW are discussed in details. A small wavelength difference

(\sim nm) is found to have negligible effects on the SP modes except for very small crossing angle ($\sim 1^\circ$). For two beams with nearly equal wavelength, wavevectors of the shared IAW of all possible collective SBS modes lie on a circle in the bisecting plane between wavevectors of the two laser beams. For a specified plasma condition, the wavelength of the scattered waves decreases with increasing beam crossing angle θ_{12} or increasing out-of-plane angle α_\perp of the SP mode. However, the strength of the SP modes are subject to more factors. Depending on the polarization states of the laser beams, and the geometry and relative orientation of the gain volume relative to the beam overlapping volume, the out-of-plane SP modes can be important. Our results suggest that in a realistic simulation for the collective SBS modes, all these factors must be properly accounted for to obtain a reliable result.

In this work, uniform plasma conditions with zero flow velocity are assumed for the illustrative analysis. However, it can be easily extended to the non-zero flow velocity case, which would lead to a wavelength shift of the scattered waves. For practical ICF conditions, the plasma inhomogeneity, together with the practical laser intensity distribution and overlapping pattern of the laser beams, would complicate the situation significantly. Accurate account of all these factors require simulations, for which this work provides valuable theoretical references. Furthermore, the analytical convective solution presented here can help construct the numerical solution by applying it over spatial regions of the grid size, as done previously for single beam LPIs [21, 29].

V. ACKNOWLEDGMENTS

This work was supported by the National Key R&D Program of China (Grant No. 2017YFA0403204), the Science Challenge Project (Grant No. TZ2016005), the National Natural Science Foundation of China (Grant No. 11875093 and 11875091), and the Development Funds of CAEP (Grant No. CX20210040).

-
- [1] J. F. Myatt, J. Zhang, R. W. Short, A. V. Maximov, W. Seka, D. H. Froula, D. H. Edgell, D. T. Michel, I. V. Igumenshchev, D. E. Hinkel, P. Michel, and J. D. Moody. Multiple-beam laser-plasma interactions in inertial confinement fusion. *Physics of Plasmas*, 21(5):055501, 2014.

- [2] R. K. Kirkwood, J. D. Moody, J. Kline, E. Dewald, S. Glenzer, L. Divol, P. Michel, D. Hinkel, R. Berger, E. Williams, J. Milovich, L. Yin, H. Rose, B. Macgowan, O. Landen, M. Rosen, and J. Lindl. A review of laser-plasma interaction physics of indirect-drive fusion. *Plasma Physics and Controlled Fusion*, 55(10):103001, 2013.
- [3] P. Michel, L. Divol, E. A. Williams, S. Weber, C. A. Thomas, D. A. Callahan, S. W. Haan, J. D. Salmonson, S. Dixit, D. E. Hinkel, M. J. Edwards, B. J. MacGowan, J. D. Lindl, S. H. Glenzer, and L. J. Suter. Tuning the implosion symmetry of icf targets via controlled crossed-beam energy transfer. *Phys. Rev. Lett.*, 102:025004, Jan 2009.
- [4] P. Michel, S. H. Glenzer, L. Divol, D. K. Bradley, D. Callahan, S. Dixit, S. Glenn, D. Hinkel, R. K. Kirkwood, J. L. Kline, W. L. Kruer, G. A. Kyrala, S. Le Pape, N. B. Meezan, R. Town, K. Widmann, E. A. Williams, B. J. MacGowan, J. Lindl, and L. J. Suter. Symmetry tuning via controlled crossed-beam energy transfer on the national ignition facility. *Physics of Plasmas*, 17(5):056305, 2010.
- [5] P. Michel, W. Rozmus, E. A. Williams, L. Divol, R. L. Berger, R. P. J. Town, S. H. Glenzer, and D. A. Callahan. Stochastic ion heating from many overlapping laser beams in fusion plasmas. *Phys. Rev. Lett.*, 109:195004, 2012.
- [6] J. D. Moody, P. Michel, L. Divol, R. L. Berger, E. Bond, D. K. Bradley, D. A. Callahan, E. L. Dewald, S. Dixit, M. J. Edwards, S. Glenn, A. Hamza, C. Haynam, D. E. Hinkel, N. Izumi, O. Jones, J. D. Kilkenny, R. K. Kirkwood, J. L. Kline, W. L. Kruer, G. A. Kyrala, O. L. Landen, S. LePape, J. D. Lindl, B. J. MacGowan, N. B. Meezan, A. Nikroo, M. D. Rosen, M. B. Schneider, D. J. Strozzi, L. J. Suter, C. A. Thomas, R. P. J. Town, K. Widmann, E. A. Williams, L. J. Atherton, S. H. Glenzer, and E. I. Moses. Multistep redirection by cross-beam power transfer of ultrahigh-power lasers in a plasma. *Nature Physics*, 8:344–349, 2012.
- [7] L. Hao, X. Y. Hu, C. Y. Zheng, B. Li, J. Xiang, and Z. J. Liu. Study of crossed-beam energy transfer process with large crossing angle in three-dimension. *Laser and Particle Beams*, 34(2):270–275, 2016.
- [8] W. Seka, H. A. Baldis, J. Fuchs, S. P. Regan, D. D. Meyerhofer, C. Stoeckl, B. Yaakobi, R. S. Craxton, and R. W. Short. Multibeam stimulated brillouin scattering from hot, solid-target plasmas. *Phys. Rev. Lett.*, 89:175002, Oct 2002.
- [9] R. K. Kirkwood, P. Michel, R. London, J. D. Moody, E. Dewald, L. Yin, J. Kline, D. Hinkel, D. Callahan, N. Meezan, E. Williams, L. Divol, B. L. Albright, K. J. Bowers, E. Bond, H. Rose,

- Y. Ping, T. L. Wang, C. Joshi, W. Seka, N. J. Fisch, D. Turnbull, S. Suckewer, J. S. Wurtele, S. Glenzer, L. Suter, C. Haynam, O. Landen, and B. J. Macgowan. Multi-beam effects on backscatter and its saturation in experiments with conditions relevant to ignition. *Physics of Plasmas*, 18(5):056311, 2011.
- [10] P. Michel, L. Divol, E. L. Dewald, J. L. Milovich, M. Hohenberger, O. S. Jones, L. Berzak Hopkins, R. L. Berger, W. L. Kruer, and J. D. Moody. Multibeam Stimulated Raman Scattering in Inertial Confinement Fusion Conditions. *Phys. Rev. Lett.*, 115(5):055003, 2015.
- [11] C. Neuville, V. Tassin, D. Pesme, M.-C. Monteil, P.-E. Masson-Laborde, C. Baccou, P. Fremerye, F. Philippe, P. Seytor, D. Teychenné, W. Seka, J. Katz, R. Bahr, and S. Depierreux. Experimental evidence of the collective brillouin scattering of multiple laser beams sharing acoustic waves. *Phys. Rev. Lett.*, 116:235002, Jun 2016.
- [12] S Depierreux, C Neuville, V Tassin, M-C Monteil, P-E Masson-Laborde, C Baccou, P Fremerye, F Philippe, P Seytor, D Teychenné, J Katz, R Bahr, M Casanova, N Borisenko, L Borisenko, A Orekhov, A Colaitis, A Debayle, G Duchateau, A Heron, S Huller, P Loiseau, P Nicolai, C Riconda, G Tran, C Stoeckl, W Seka, V Tikhonchuk, D Pesme, and C Labaune. Experimental investigation of the collective stimulated brillouin and raman scattering of multiple laser beams in inertial confinement fusion experiments. *Plasma Physics and Controlled Fusion*, 62(1):014024, dec 2019.
- [13] D. F. DuBois, Bandel Bezzerides, and Harvey A. Rose. Collective parametric instabilities of many overlapping laser beams with finite bandwidth. *Physics of Fluids B: Plasma Physics*, 4(1):241–251, 1992.
- [14] C. Z. Xiao, H. B. Zhuo, Y. Yin, Z. J. Liu, C. Y. Zheng, and X. T. He. Linear theory of multibeam parametric instabilities in homogeneous plasmas. *Physics of Plasmas*, 26(6):062109, 2019.
- [15] Yao Zhao, Charles F Wu, Su-Ming Weng, Zheng-Ming Sheng, and Jianqiang Zhu. Mitigation of multibeam stimulated raman scattering with polychromatic light. *Plasma Physics and Controlled Fusion*, feb 2021.
- [16] D. W. Forslund, J. M. Kindel, and E. L. Lindman. Theory of stimulated scattering processes in laser-irradiated plasmas. *Physics of Fluids*, 18(8):1002–1016, 1975.
- [17] Liang Hao, Yiqing Zhao, Dong Yang, Zhanjun Liu, Xiaoyan Hu, Chunyang Zheng, Shiyang Zou, Feng Wang, Xiaoshi Peng, Zhichao Li, Sanwei Li, Tao Xu, and Huiyue Wei. Analysis of

- stimulated raman backscatter and stimulated brillouin backscatter in experiments performed on sg-iii prototype facility with a spectral analysis code. *Physics of Plasmas*, 21(7):072705, 2014.
- [18] Liang Hao, Dong Yang, Xin Li, Zhichao Li, Yaoyuan Liu, Hongbo Cai, Zhanjun Liu, Peijun Gu, Tao Xu, Sanwei Li, Bin Li, Minqing He, Sizhong Wu, Qiang Wang, Lihua Cao, Chunyang Zheng, Weiyi Zha, Xiaoshi Peng, Yonggang Liu, Yulong Li, Xiangming Liu, Pin Yang, Liang Guo, Xiaohua Jiang, Lifei Hou, Bo Deng, Peng Wang, Shenye Liu, Jiamin Yang, Feng Wang, Wudi Zheng, Shiyang Zou, Jie Liu, Shaoen Jiang, Yongkun Ding, and Shaoping Zhu. Investigation on laser plasma instability of the outer ring beams on sgiii laser facility. *AIP Advances*, 9(9):095201, 2019.
- [19] Yu Ji, Chang-Wang Lian, Rui Yan, Chuang Ren, Dong Yang, Zhen-Hua Wan, Bin Zhao, Chen Wang, Zhi-Heng Fang, and Jian Zheng. Convective amplification of stimulated raman rescattering in a picosecond laser plasma interaction regime. *Matter and Radiation at Extremes*, 6(1):015901, 2021.
- [20] S. J. Yang, H. B. Zhuo, Y. Yin, Z. J. Liu, C. Y. Zheng, X. T. He, and C. Z. Xiao. Growth and saturation of stimulated raman scattering in two overlapping laser beams. *Phys. Rev. E*, 102:013205, 2020.
- [21] D. J. Strozzi, E. A. Williams, D. E. Hinkel, D. H. Froula, R. A. London, and D. A. Callahan. Ray-based calculations of backscatter in laser fusion targets. *Physics of Plasmas*, 15(10):102703, 2008.
- [22] P. Michel, W. Rozmus, E. A. Williams, L. Divol, R. L. Berger, S. H. Glenzer, and D. A. Callahan. Saturation of multi-laser beams laser-plasma instabilities from stochastic ion heating. *Physics of Plasmas*, 20(5):056308, 2013.
- [23] Yao Zhao, Suming Weng, Min Chen, Jun Zheng, Hongbin Zhuo, and Zhengming Sheng. Stimulated raman scattering excited by incoherent light in plasma. *Matter and Radiation at Extremes*, 2(4):190 – 196, 2017.
- [24] Yao Zhao, Suming Weng, Zhengming Sheng, and Jianqiang Zhu. Suppression of parametric instabilities in inhomogeneous plasma with multi-frequency light. *Plasma Physics and Controlled Fusion*, 61(11):115008, 2019.
- [25] P. Michel, L. Divol, R. P. J. Town, M. D. Rosen, D. A. Callahan, N. B. Meezan, M. B. Schneider, G. A. Kyrala, J. D. Moody, E. L. Dewald, K. Widmann, E. Bond, J. L. Kline, C. A.

- Thomas, S. Dixit, E. A. Williams, D. E. Hinkel, R. L. Berger, O. L. Landen, M. J. Edwards, B. J. MacGowan, J. D. Lindl, C. Haynam, L. J. Suter, S. H. Glenzer, and E. Moses. Three-wavelength scheme to optimize hohlraum coupling on the national ignition facility. *Phys. Rev. E*, 83:046409, Apr 2011.
- [26] Antonio Corvo and Athanasios Gavrielides. Forward stimulated brillouin scattering. *Journal of Applied Physics*, 63(11):5220–5227, 1988.
- [27] C. J. McKinstrie, J. S. Li, and A. V. Kanaev. Near-forward stimulated brillouin scattering. *Physics of Plasmas*, 4(12):4227–4231, 1997.
- [28] David S. Montgomery. Two decades of progress in understanding and control of laser plasma instabilities in indirect drive inertial fusion. *Physics of Plasmas*, 23(5):055601, 2016.
- [29] B. Bezzerides, H. X. Vu, and J. M. Wallace. Convective gain of stimulated brillouin scattering in long-scale length, two-ion-component plasmas. *Physics of Plasmas*, 3(3):1073–1090, 1996.
- [30] E. A. Williams, R. L. Berger, R. P. Drake, A. M. Rubenchik, B. S. Bauer, D. D. Meyerhofer, A. C. Gaeris, and T. W. Johnston. The frequency and damping of ion acoustic waves in hydrocarbon (ch) and two-ion-species plasmas. *Physics of Plasmas*, 2(1):129–138, 1995.
- [31] Joyati Debnath and R.S. Dahiya. Theorems on multidimensional laplace transform for solution of boundary value problems. *Computers and Mathematics with Applications*, 18(12):1033 – 1056, 1989.

Appendix A: Properties of ponderomotive response function

For the shared IAW modes of SBS, one critical factor that appears in the gain coefficients is

$$k_a^2 \text{Im}[\gamma_{\text{pm}}] = k_a^2 \text{Im}\left[\frac{(1 + \chi_I)\chi_e}{1 + \chi_I + \chi_e}\right] \quad (\text{A1})$$

The peak value of $k_a^2 \text{Im}[\gamma_{\text{pm}}]$ is achieved near the naturally resonant IAW modes where $\epsilon = 1 + \chi_I + \chi_e \approx 0$ and $\omega_a = k_a c_s$ with c_s being the ion acoustic velocity. Since $1 + \chi_I + \chi_e \approx 0$, the peak value satisfies

$$\max[k_a^2 \text{Im}[\gamma_{\text{pm}}]] \approx \frac{k_a^2 |\chi_e|^2}{(\partial \epsilon_r / \partial \omega) \nu_a}, \quad (\text{A2})$$

which is inversely proportional to the damping rate (ν_a) of IAW. Here ϵ_r is the real part of ϵ . It is found that the peak value of $k_a^2 \text{Im}[\gamma_{\text{pm}}]$ increases (weakly) with decreasing k_a , and the half-width of $k_a^2 \text{Im}[\gamma_{\text{pm}}]$ which is proportional to the damping is anti-correlated with the

peak value of $k_a^2 \text{Im}[\gamma_{\text{pm}}]$. This can be illustrated in the fluid limit $v_{\text{the}} \gg c_s \gg v_{\text{thI}}$, where v_{the} and v_{thI} are the electron and ion thermal velocity respectively, and there are relatively simple analytical formulae for χ_I and χ_e . In the fluid limit,

$$\max[k_a^2 \text{Im}[\gamma_{\text{pm}}]] = \frac{\omega_{\text{pi}}^2 \omega_a}{2c_s^2 \nu_a}, \quad (\text{A3})$$

where ω_{pi} is the ion plasma frequency. For He plasma with Maxwellian EEDF, the ion acoustic velocity [30] is given by

$$c_s = \sqrt{\frac{ZT_e}{m_i}} \sqrt{\frac{1}{1 + k_a^2 \lambda_{\text{De}}^2} + \frac{3T_i}{ZT_e}}, \quad (\text{A4})$$

Using the approximation $\nu_a = \text{Im}[\epsilon]/(\partial\epsilon_r/\partial\omega)$, it can be obtained

$$\frac{\nu_a}{\omega_a} = \sqrt{\frac{\pi}{8(1 + k_a^2 \lambda_{\text{De}}^2)^3}} \left[\left(\frac{ZT_e}{T_i}\right)^{3/2} \exp\left(-\frac{c_s^2}{2v_{\text{thI}}^2}\right) + \sqrt{\frac{Zm_e}{m_i}} \right]. \quad (\text{A5})$$

So with the decrease of k_a , c_s (weakly) increases, and hence the exponential part (corresponding to the tail of the ion energy distribution function) of ν_a/ω_a decreases. The change in the exponential part is generally stronger, leading to decreasing ν_a/ω_a and $c_s^2 \nu_a/\omega_a$ with decreasing k_a . As a consequence, $\max[k_a^2 \text{Im}[\gamma_{\text{pm}}]]$ as given by Eq. (A3) increases (slowly) with decreasing k_a .

Appendix B: Convective solution for the SP modes of two crossing beams by the two-dimensional Laplace transformation

The two-dimensional Laplace transform of a function $f(x, y)$ [31] is defined by

$$\mathcal{L}_{\mathbf{q}}[f(x, y)] \equiv \int_0^\infty \int_0^\infty f(x, y) e^{-q^x x - q^y y} dx dy \quad (\text{B1})$$

where $\mathbf{q} = (q^x, q^y)$, and q^x and q^y are the complex frequencies corresponding to x_1 and x_2 , respectively. The associated one-dimensional Laplace transforms along x -axis and y -axis are defined by

$$\mathcal{L}_{q^x}[f(x)] \equiv \int_0^\infty f(x) e^{-q^x x} dx \quad (\text{B2})$$

$$\mathcal{L}_{q^y}[f(y)] \equiv \int_0^\infty f(y) e^{-q^y y} dy. \quad (\text{B3})$$

The Laplace transform changes differentiation to multiplication,

$$\mathcal{L}_{\mathbf{q}}[\partial_x f(x, y)] = q^x \mathcal{L}_{\mathbf{q}}[f(x, y)] - \mathcal{L}_{q^y}[f(x = 0, y)] \quad (\text{B4})$$

$$\mathcal{L}_{\mathbf{q}}[\partial_y f(x, y)] = q^y \mathcal{L}_{\mathbf{q}}[f(x, y)] - \mathcal{L}_{q^x}[f(x, y = 0)] \quad (\text{B5})$$

When $\mathcal{L}_{\mathbf{q}}[f(x, y)]$ is known, $f(x, y)$ can be restored by the inverse Laplace transform,

$$f(x, y) = \mathcal{L}_{\mathbf{q}}^{-1}\{\mathcal{L}_{\mathbf{q}}[f(x, y)]\}. \quad (\text{B6})$$

The operation of $\mathcal{L}_{\mathbf{q}}^{-1}$ on the one-dimensional Laplace transforms yields

$$\mathcal{L}_{\mathbf{q}}^{-1}\{\mathcal{L}_{q^x}[f(x)]\} = \delta(y)f(x) \quad (\text{B7})$$

$$\mathcal{L}_{\mathbf{q}}^{-1}\{\mathcal{L}_{q^y}[f(y)]\} = \delta(x)f(y)$$

The inverse Laplace transform changes convolution into multiplication,

$$\mathcal{L}_{\mathbf{q}}^{-1}[G_1(\mathbf{q})G_2(\mathbf{q})] = \mathcal{L}_{\mathbf{q}}^{-1}[G_1(\mathbf{q})] * \mathcal{L}_{\mathbf{q}}^{-1}[G_2(\mathbf{q})] \quad (\text{B8})$$

where the symbol ‘*’ denotes the convolution operation defined as

$$(f * g)(x, y) = \int_0^x \int_0^y f(u, v)g(x - u, y - v)dudv \quad (\text{B9})$$

Using Eqs. (B4-B5), the two-dimensional Laplace transform of Eqs. (15-16) over the (x_1, x_2) -space can be written as

$$q^{x_1} \mathcal{L}_{\mathbf{q}}[a_{s_1}] - F_1 = \kappa_1(\mathcal{L}_{\mathbf{q}}[a_{s_1}] + r_a \mathcal{L}_{\mathbf{q}}[a_{s_2}]) \quad (\text{B10})$$

$$q^{x_2} \mathcal{L}_{\mathbf{q}}[a_{s_2}] - F_2 = \kappa_2(\mathcal{L}_{\mathbf{q}}[a_{s_2}] + \mathcal{L}_{\mathbf{q}}[a_{s_1}]/r_a) \quad (\text{B11})$$

where

$$F_1 \equiv \mathcal{L}_{q^{x_2}}[a_{s_1}(x_1 = 0, x_2)] \quad (\text{B12})$$

$$F_2 \equiv \mathcal{L}_{q^{x_1}}[a_{s_2}(x_1, x_2 = 0)]$$

is determined by the boundary conditions specified by $a_{s_1}(x_1 = 0, x_2)$ and $a_{s_2}(x_1, x_2 = 0)$.

Solving for $\mathcal{L}_{\mathbf{q}}[a_{s_1}]$ and $\mathcal{L}_{\mathbf{q}}[a_{s_2}]$, we obtain

$$\mathcal{L}_{\mathbf{q}}[a_{s_1}] = \frac{(q^{x_2} - \kappa_2)F_1 + \kappa_1 r_a F_2}{q^{x_1} q^{x_2} - \kappa_1 q^{x_2} - \kappa_2 q^{x_1}} \quad (\text{B13})$$

$$\mathcal{L}_{\mathbf{q}}[a_{s_2}] = \frac{(q^{x_1} - \kappa_1)F_2 + \kappa_2 F_1 / r_a}{q^{x_1} q^{x_2} - \kappa_1 q^{x_2} - \kappa_2 q^{x_1}}. \quad (\text{B14})$$

Then, a_{s_1} and a_{s_2} can be restored from $\mathcal{L}_{\mathbf{q}}[a_{s_1}]$ and $\mathcal{L}_{\mathbf{q}}[a_{s_2}]$ by the inverse Laplace transform. Using the identities (B6-B8), it can be obtained

$$\begin{bmatrix} a_{s_1}(x_1, x_2) \\ a_{s_2}(x_1, x_2) \end{bmatrix} = \int_0^{x_2} \mathbf{G}_1(x_1, x_2 - v) a_{s_1}(x_1 = 0, v) dv + \int_0^{x_1} \mathbf{G}_2(x_1 - u, x_2) a_{s_2}(u, x_2 = 0) du \quad (\text{B15})$$

where

$$\mathbf{G}_1(x_1, x_2) = \begin{bmatrix} G_{11} \\ G_{21} \end{bmatrix} = \begin{bmatrix} \kappa_2 \kappa_1 x_1 e^{\kappa_1 x_1 + \kappa_2 x_2} \frac{I_1[2\sqrt{\kappa_1 \kappa_2 x_1 x_2}]}{\sqrt{\kappa_1 \kappa_2 x_1 x_2}} \\ (\kappa_2/r_a) e^{\kappa_1 x_1 + \kappa_2 x_2} I_0[2\sqrt{\kappa_1 \kappa_2 x_1 x_2}] \end{bmatrix} + \begin{bmatrix} e^{\kappa_1 x_1} \delta(x_2) \\ 0 \end{bmatrix}, \quad x_1 \geq 0, x_2 \geq 0 \quad (\text{B16})$$

and

$$\mathbf{G}_2(x_1, x_2) = \begin{bmatrix} G_{12} \\ G_{22} \end{bmatrix} = \begin{bmatrix} r_a \kappa_1 e^{\kappa_1 x_1 + \kappa_2 x_2} I_0[2\sqrt{\kappa_1 \kappa_2 x_1 x_2}] \\ \kappa_1 \kappa_2 x_2 e^{\kappa_1 x_1 + \kappa_2 x_2} \frac{I_1[2\sqrt{\kappa_1 \kappa_2 x_1 x_2}]}{\sqrt{\kappa_1 \kappa_2 x_1 x_2}} \end{bmatrix} + \begin{bmatrix} 0 \\ e^{\kappa_2 x_2} \delta(x_1) \end{bmatrix}, \quad x_1 \geq 0, x_2 \geq 0 \quad (\text{B17})$$

Appendix C: The representative direction \mathbf{n}_A and the representative gain coefficient

κ_A

The direction of \mathbf{n}_A satisfies $\mathbf{n}_A \parallel \nabla G_A$, where the asymptotic gain coefficient $G_A = e^{(\sqrt{\kappa_1 x_1} + \sqrt{\kappa_2 x_2})^2}$. To obtain the direction of \mathbf{n}_A , it is convenient to rewrite G_A in an orthogonal coordinate system. Defining the \tilde{x}_1 -axis along \mathbf{n}_{s_1} and \tilde{x}_2 -axis perpendicular to \mathbf{n}_{s_1} , the transformation between (x_1, x_2) and $(\tilde{x}_1, \tilde{x}_2)$ is given by $x_1 = (\tilde{x}_1 \sin \theta_{12}^s - \tilde{x}_2 \cos \theta_{12}^s) / \sin \theta_{12}^s$ and $x_2 = \tilde{x}_2 / \sin \theta_{12}^s$. The condition $\mathbf{n}_A \parallel \nabla G_A$ gives us

$$\frac{\partial G / \partial \tilde{x}_1}{\partial G / \partial \tilde{x}_2} = \frac{\tilde{x}_1}{\tilde{x}_2}, \quad (\text{C1})$$

After some manipulation, the relation between $x_r \equiv x_2/x_1$ and $\kappa_r \equiv \kappa_2/\kappa_1$ can be obtained,

$$\frac{(x_r + \cos \theta_{12}^s) \sqrt{x_r}}{1 + x_r \cos \theta_{12}^s} = \sqrt{\kappa_r}. \quad (\text{C2})$$

Correspondingly, the angle between \mathbf{n}_A and \mathbf{n}_{s_1} is

$$\cos \theta_A = \frac{1 + x_r \cos \theta_{12}^s}{\sqrt{1 + x_r^2 + 2x_r \cos \theta_{12}^s}}. \quad (\text{C3})$$

At the point $\mathbf{x} = x_1(\mathbf{n}_{s_1} + x_r \mathbf{n}_{s_2})$ along the direction \mathbf{n}_A , $G_A = \exp[(1 + \sqrt{\kappa_r x_r})^2 \kappa_1 x_1]$, and the required 2D gain volume is the parallelogram $x_1(\eta_1 \mathbf{n}_{s_1} + \eta_2 x_r \mathbf{n}_{s_2})$ ($0 \leq \eta_{1,2} \leq 1$). The

two diagonals of the parallelogram have lengths $x_1\sqrt{1+x_r^2 \pm 2x_r \cos \theta_{12}^s}$. Using the root mean square of the two diagonals as the typical size (L_m) of the required gain volume, we have $L_m = x_1\sqrt{1+x_r^2}$, and the gain coefficient $\kappa_A \equiv \ln G_A/L_m$ defined for this typical size satisfies

$$\mathcal{R}_A[\kappa_r, \theta_{12}^s] \equiv \frac{\kappa_A}{\kappa_1 + \kappa_2} = \frac{(1 + \sqrt{\kappa_r x_r})^2}{(1 + \kappa_r)\sqrt{1 + x_r^2}}. \quad (\text{C4})$$

The ratio \mathcal{R}_A is a function of κ_r and θ_{12}^s , since x_r in the RHS is a function of κ_r and θ_{12}^s as specified by Eq. (C2). \mathcal{R}_A varies between 1 and $\sqrt{2}$. The upper bound of $\sqrt{2}$ appears with \mathbf{n}_A along the bisector of \mathbf{n}_{s_1} and \mathbf{n}_{s_2} when $\kappa_1 = \kappa_2$ and hence $x_1 = x_2$, while the lower bound of one can be approached when $\kappa_1 \ll \kappa_2$ or $\kappa_2 \ll \kappa_1$.

Appendix D: The projection of the gain volume onto one direction \mathbf{n}_r and perpendicular to \mathbf{n}_r

The parallelogram gain volume $V_{\text{amp}}(\mathbf{x}) = \eta_1 x_1 \mathbf{n}_{s_1} + \eta_2 x_2 \mathbf{n}_{s_2}$ ($0 \leq \eta_{1,2} \leq 1$) is spanned by \mathbf{n}_{s_1} and \mathbf{n}_{s_2} . Denoting the projection of \mathbf{n}_{s_α} onto one direction \mathbf{n}_r as $\mathbf{n}_{s_\alpha}^{\parallel \mathbf{n}_r}$, and the projection of \mathbf{n}_{s_α} onto the plane perpendicular to \mathbf{n}_r as $\mathbf{n}_{s_\alpha}^{\perp \mathbf{n}_r}$, then

$$\mathbf{n}_{s_\alpha} = \mathbf{n}_{s_\alpha}^{\parallel \mathbf{n}_r} + \mathbf{n}_{s_\alpha}^{\perp \mathbf{n}_r}, \quad (\text{D1})$$

yielding

$$\begin{aligned} V_{\text{amp}} &= V_{\text{amp}}^{\parallel \mathbf{n}_r} + V_{\text{amp}}^{\perp \mathbf{n}_r}, \\ V_{\text{amp}}^{\parallel \mathbf{n}_r} &\equiv x_1 \eta_1 \mathbf{n}_{s_1}^{\parallel \mathbf{n}_r} + x_2 \eta_2 \mathbf{n}_{s_2}^{\parallel \mathbf{n}_r} \\ V_{\text{amp}}^{\perp \mathbf{n}_r} &\equiv x_1 \eta_1 \mathbf{n}_{s_1}^{\perp \mathbf{n}_r} + x_2 \eta_2 \mathbf{n}_{s_2}^{\perp \mathbf{n}_r} \end{aligned} \quad (\text{D2})$$

It can be seen that the longitude scale of the gain volume defined as the length of $V_{\text{amp}}^{\parallel \mathbf{n}_r}$ is $\text{Proj}_{\parallel \mathbf{n}_r}[V_{\text{amp}}] = x_1 |\mathbf{n}_{s_1}^{\parallel \mathbf{n}_r}| + x_2 |\mathbf{n}_{s_2}^{\parallel \mathbf{n}_r}|$ for $\eta_{1,2}$ ranging from zero to one. While $V_{\text{amp}}^{\perp \mathbf{n}_r}$ is itself a parallelogram in the plane perpendicular to n_r , so the transverse scale of the gain volume defined as the longest spatial scale of $V_{\text{amp}}^{\perp \mathbf{n}_r}$ is the longer diagonal, $\text{Proj}_{\perp \mathbf{n}_r}[V_{\text{amp}}] = \sqrt{x_1^2 |\mathbf{n}_{s_1}^{\perp \mathbf{n}_r}|^2 + x_2^2 |\mathbf{n}_{s_2}^{\perp \mathbf{n}_r}|^2 + 2x_1 x_2 |\mathbf{n}_{s_1}^{\perp \mathbf{n}_r} \cdot \mathbf{n}_{s_2}^{\perp \mathbf{n}_r}|}$.